cogent geoscience

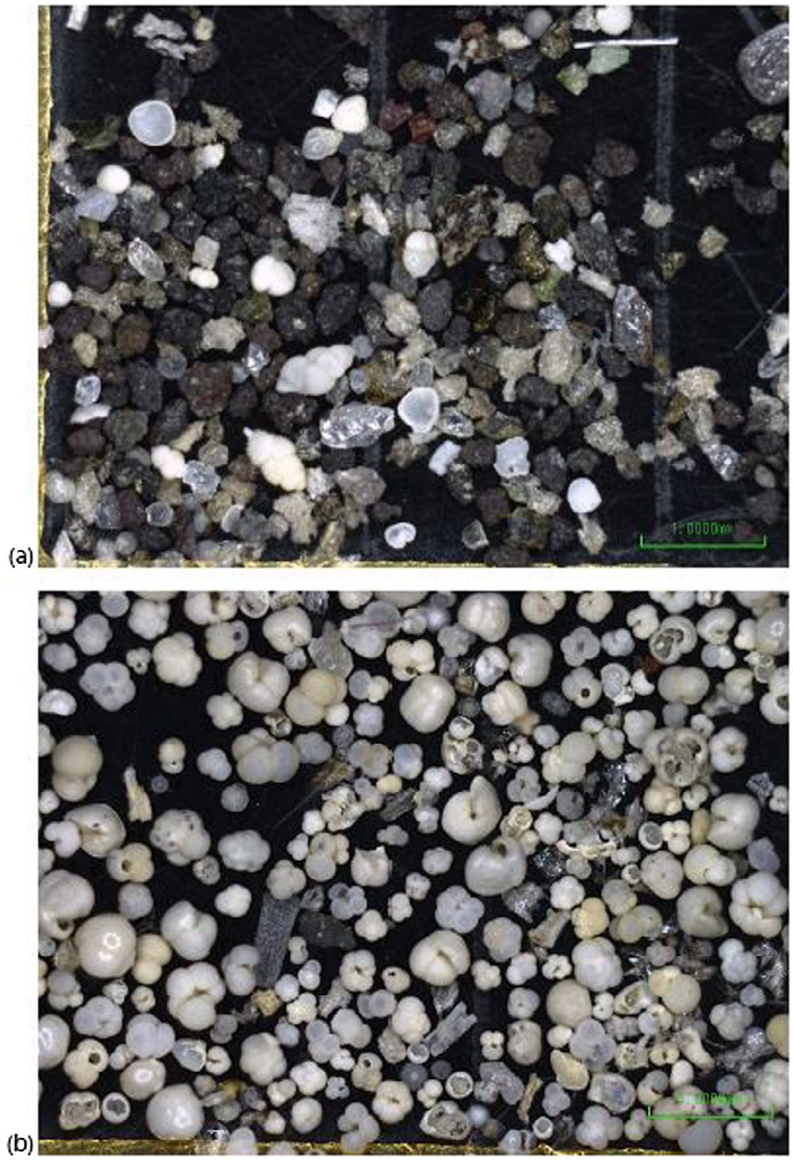

HYDROSPHERE | RESEARCH ARTICLE

Quantitative planktonic foraminifers taphonomy and palaeoceanographic implications over the last 1 My from IODP Sites U1436 and U1437

Maryline J. Mleneck-Vautravers

Cogent Geoscience (2018), 4: 1447263

cogent geoscience

HYDROSPHERE | RESEARCH ARTICLE

Quantitative planktonic foraminifers taphonomy and palaeoceanographic implications over the last 1 My from IODP Sites U1436 and U1437

Maryline J. Mleneck-Vautravers[1]*

Received: 29 October 2017
Accepted: 18 February 2018
First Published: 03 March 2018

*Corresponding author: Maryline J. Mleneck-Vautravers, Godwin Laboratory for Palaeoclimate Research, Department of Earth Sciences, University of Cambridge, Downing Street, Cambridge CB2 3EQ, UK
E-mail: mv217@cam.ac.uk

Reviewing editor:
Gabriella Bagnoli, Universita di Pisa, Italy

Additional information is available at the end of the article

Abstract: International Ocean Discovery Program Sites U1437 and U1436, two intermediate water depth sites located near the Kuroshio Current were studied for planktonic proxies, shell weights, percent fragments, foraminifers concentrations, and benthic/planktonic ratios. Over the last 1 My, the foraminifers assemblages responded to local temperature changes. The taphonomy of these assemblages limits their usefulness as palaeoclimatic records but greatly inform qualitatively of intermediate water mass changes on each side of the Izu Rise. Carbonate dissolution (CD) is pervasive and always more intense during interglacials at the shallowest Site U1436 to the East. Carbonate preservation improved during glacials after 0.6 Ma at U1437B (West) likely signaling changes within the glacial Antarctic Intermediate Water and therefore, its source water the Glacial North Atlantic Intermediate Water from Marine Isotope Stage 16. The first occurrence of a very large Laurentide ice-sheet at the time is proposed as a potential indirect cause for this observation. Both the intensification of carbonate dissolution during each interglacials from MIS17 onwards and the better preservation during succeeding glacials after that are attributed to the increasing influence of the North Atlantic Deep Water and the Glacial North Atlantic Intermediate Water via the Antarctic Intermediate Water during Interglacial and Glacial intervals, respectively.

Maryline J. Mleneck-Vautravers

ABOUT THE AUTHOR

Maryline J. Mleneck-Vautravers is a chief senior research technician based in the Godwin Laboratory for Paleoclimate Research. She has more than 20 years of experience in Paleoceanography and is specialized in the study of marine microfossils called foraminifers and their preservation state. Foraminifers are widely used to reconstruct Earth's climate over the last 65 Ma using a range of paleontological and geochemical methods.

PUBLIC INTEREST STATEMENT

Deep-sea carbonates accumulate on most parts of the ocean floor after the death of planktonic foraminifers forming a large reservoir of carbon and are a key part of the carbon cycle responding to dissolved carbon content in the ocean. The later in turn interacts with the atmosphere, which holds a small reservoir of carbon (CO_2). During the last million years, the concentration of atmospheric CO_2 varied between high values during warm intervals (interglacials) and low values during glacial intervals. I examined two long sedimentary cores recovered via deep-sea drilling at intermediate water depth South of Japan. I show, that Glacials contain better preserved carbonate than interglacials. This tendency became stronger after glacial intervals became more intense after 650,000 years ago. The cause for this observation could be linked to increasing ice volume over certain parts of the northern hemisphere after this date and being transferred via influence on intermediate water masses globally.

Subjects: Palaeontology; Palaeoceanography; Micropalaeontology

Keywords: planktonic foraminifers; calcium carbonate cycles; intermediate water depth circulation; Middle Pleistocene transition

1. Introduction

Because of its relatively fresh surface waters, the North Pacific Ocean unlike the North Atlantic is not the site of deep-convection that could lead to the formation of a North Pacific deep-water mass. Not at the source of any deep-circulation and sited at the "end of the line" of the global ocean circulation, the North Pacific contains the oldest and the least ventilated (i.e. very high total CO_2, high nutrients; P, N, Si, and very low O_2) water on Earth. In contrast, the North Pacific Intermediate Water Mass (NPIW; Talley, 1993) is formed via mixing of the salty subtropical Kuroshio and the fresher Oyashio currents waters in the mixed water area (Talley et al., 1995). This water mass is clearly visible on the World Ocean Circulation Experiment section profiles (Talley, 2007), particularly through the low salinity and low O_2 concentrations centered above 1,500 meters water depth along the sections in this area. Such style of circulation makes the Pacific Ocean a hostile environment for calcium carbonate preservation. It has long been observed that the North Pacific lysocline (i.e. the depth at which the carbonate content decreases dramatically in deep-sea sediments) is the shallowest on Earth (Arhenius, 1953) and that carbonate dissolution there is very intense during interglacial intervals (Farrell & Prell, 1989). The later contrasts with the Atlantic Ocean where sediments are better preserved during interglacial intervals. This observation gives way to the notion of contrasted carbonate preservation styles between oceanic basins at glacial–interglacial timescales. Current, hypotheses about intensity changes in the formation of NPIW during glacial/interglacial stages point to intensified glacial production whilst the North Atlantic Deep Water (NADW) production is re-intensified during the deglaciation (Galbraith et al., 2007). The Pacific Ocean experiences cyclic changes in the preservation of deep-sea carbonate or "$CaCO_3$ cycles", which simply means that its water was less acidic during glacials and accumulated more $CaCO_3$ at greater depths than during interglacials (Arhenius, 1953; Farrell & Prell, 1989; Le & Shackleton, 1992).

The general understanding of the driver behind the observed Pacific vs. Atlantic carbonate cycles pattern (i.e. in the Atlantic deep-sea carbonate are better preserved during Interglacials) is presented by Hodell, Charles, and Sierro (2001) but is mostly concerned with the deepest branch of the deep global circulation, swinging between Antarctic Bottom Water (AABW) and Lower North Atlantic Deep Water (LNADW) in the deepest part of the South Atlantic and does not examine the Pacific Ocean.

During IODP Expedition 350 two sites, U1436 and U1437 were cored in the Western Pacific Ocean and the Philippine Sea, respectively. Both are within the influence Kuroshio Current, at the intermediate water depth of 1,717 and 2,117 m, respectively (Figure 1). U1437B drilled with primary objectives "the rear-arc evolution" (Tamura et al., 2015) is a 1,800 m long section consisting mostly of mud and mud with ash and tuffs. The sedimentary body is under the influence of the Antarctic Intermediate Water (AAIW), which circulates in the Shikhoku Basin and the Kuroshio Current at the surface. The section especially, the upper 1 My (Kars et al., 2017; Tamura et al., 2015) can therefore be used to reconstruct a record of the fluctuating influences of the warm Kuroshio (KC) vs. that of the cold Oyashio (OC) surface currents using quantitative study of the planktonic foraminifers or other geochemical methods. Crucially, the micropalaeontological data can also be used to approach qualitative changes within intermediate depth water masses through time with respect to carbonate saturation. U1436C was cored as a short (150 m) geotechnical hole. The site yields a complete record of Late Pleistocene fore-arc sedimentation influenced by frontal arc explosive volcanism (Tamura et al., 2015; Vautravers et al., 2016) and provides an opportunity to investigate the history of Late Pleistocene volcanism near the volcanic island of Aogashima. However, regarding intermediate water the shallowest U1436C on the East Site of the arc is more influenced by the NPIW than by the AAIW. This study aims to provides an evaluation of the changes affecting the Pacific Ocean intermediate deep-water masses and their effect on the record of calcium carbonate preservation,

Figure 1. Location.

Notes: Map of the North Pacific Ocean with locations of Exp350 sites: U1436C and U1437B (red dots).
Source: Tamura et al. (2015).

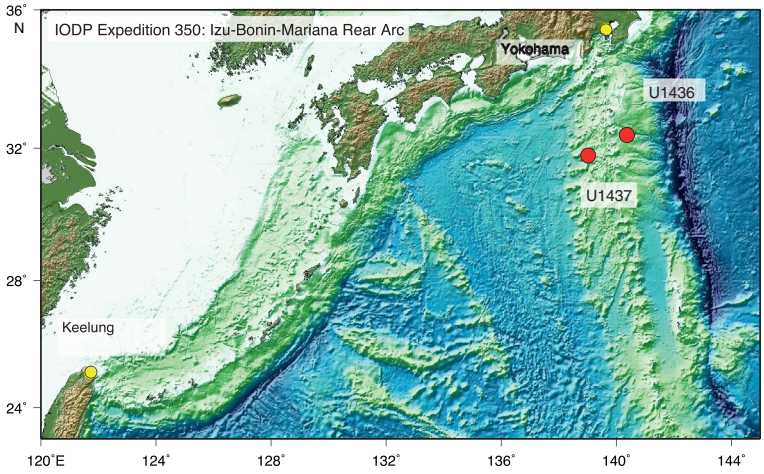

which is a first for two sites such as U1436 and U1437 also informing on the Quaternary climatic evolution because of the tight coupling between the changes in the lysocline depth and the atmospheric CO_2 concentrations (Zeebe & Marchitto, 2010). This situation arises from the scarcity of expanded sections in the Pacific Ocean where sedimentation rates are usually low because of either the distance from detrital sources, the intense biogenic carbonate dissolution or the combination of both. The present study documents the last 1 My on the basis of isotopic data and stratigraphy (Kars et al., 2017; Schindlbeck et al., 2018; Vautravers et al., 2016) also covering the Mid-Pleistocene Transition (MPT, c. 1–0.6 Ma) when the rhythm of global climatic cycles changed from mostly 40 Kyrs cycle to mostly 100 Kyrs cycles. Large palaeoenvironmental changes occurred in the Atlantic Ocean around this time and were recorded at the surface and in the deep water (Hodell, Channell, Curtis, Romero, & Röhl, 2008). Poirier and Billups (2014) examining the changing influences in deep North and deep South waters via the changes in $\delta^{13}C$ over the MPT and attributed the changes (i.e. increasing $\delta^{13}C$) on cooling in sub-polar surface water in the North Atlantic ocean from MIS17 onwards leading to a larger production of NADW. The potential for similar and co-existing changes in the western, subtropical North Pacific Ocean have not been sufficiently explored despite the major role generally attributed to Western surface boundary currents. Such surface current contributes to moisture and heat transfers towards the pole, where via moisture supply they affect the climate in sub-polar latitudes, helping ice-sheet nucleation and growth during glacial inceptions (Driscoll & Haug, 1998) and North Pacific Western Boundary current circulation changes could have resulted in intermediate depth circulation changes.

2. Regional settings

2.1. Surface currents

The subtropical NW Pacific Ocean circulation in the area studies is mostly governed by the occurrence of the eastward-flowing Kuroshio Current. Regional physical oceanography (Qui, 2001) shows that the KC path South of Japan is bimodal with its larger meander moving southward in relation to decreasing transport during ENSO events (He & White, 1987; White & McCreary, 1976). Therefore, both the warm Western Pacific pool via the KC or cooling in the polar and sub-polar parts of the North Pacific Ocean via the Oyashio current can affect the sites.

2.2. Intermediates water masses

Investigating the formation and circulation of the NPIW, Talley (1993) identified in the area of mixing between the cold sub-polar Oyashio current and the warm but fresh water from the Tsushima Current water exiting the Japan Sea as the source of the NPIW following winter cooling and sinking. Mid-Western Pacific transect WOCE P14 (Talley, 2007) shows based on oxygen concentration that this water mass is centered at ~1,500 meters water depth and extends to latitudes as South as 10°S. NPIW does not mix with the other low salinity intermediate water (AAIW) traveling North at a similar

water depth. Before reaching northwards in all oceans, the AAIW forms around Antarctica from the upwelled water originating in the North Atlantic Ocean (i.e. the NADW) and traveling at great depth (>3,000 m) before resurfacing under the influence of the strong Westerlies around Antarctica (Orsi, Whitworth, & Worth, 1995). Therefore, the formation of AAIW results directly from the conversion of a deep-water mass (NADW) into an intermediate water mass (AAIW) carrying some of the preformed properties. Such a conversion has operated at various intensities in the past (Pahnke & Zahn, 2005). The striking difference between the NPIW and the AAIW is that the AAIW carries into the Pacific preformed properties acquired in the North Atlantic as a young ventilated water mass with low nutrients, high oxygen contents and high $\delta^{13}C$, whereas the NPIW forms locally in the North Pacific as an "end of the line" water mass incorporating low oxygen, high nutrients, high respired CO_2 contents and low $\delta^{13}C$ due to the accumulating effect of the organic matter remineralization. The North Pacific Ocean (i.e. NPIW) acts as a Carbon trap, removing it from the atmosphere and storing it into the dissolved pool especially when global circulation is reduced. Some of this carbon is then released into the atmosphere during glacial termination at the time of re-invigoration of global circulation (Galbraith et al., 2007).

3. Background for sites U1436 and U1437

U1437B (31°47.39′N and 139°01.57′E; 2,117 meters water depth) West of the Izu rise, which creates a hydrographic divide at intermediate depth (Talley, 2007). U1436C (32°23.87′N and 140°21.92′E; 1,774 meters water depth) sits on the East side of the rise at the front of the arc (Figure 1, adapted from the transit map of Exp IODP 350 in 2014, Tamura et al., 2015).

The material at U1437 accumulates in a small basin with high sedimentation rates between two volcanic chains. U1436 has accumulated less pelagic sediments than U1437 and more volcaniclastic ones because of its proximity to an active submarine volcano (Tamura et al., 2015). Despite being both in the Izu-Bonin area their volcanologic history affects the sedimentation rates in contrasted manners. U1436 receives copious ashes from nearby Aogashima Caldera, whereas U1437 more distal tends to receive only the finest volcaniclastics from distant volcanoes dispersed by winds.

4. Material and methods

4.1. Sampling strategy

Samples from Hole U1437B span cores 1H through 18F (0–122 mbsf). The 205 samples covering the last 1 My are spaced at an average of 0.4 m based on biostratigraphy (Tamura et al., 2015) and confirmed by stable isotopes (Kars et al., 2017; Schindlbeck et al., 2018). Similarly for Hole U1436C, 195 samples spanning cores 1H through 18F (0–70) mbsf are included, (Vautravers et al., 2016) the samples cover the last 0.9 My. Both sites are studied at a variable but similar time resolution between a few thousands to a few 10 kyrs.

4.2. Sample preparation

Coarse fractions preparation used a standard wet-sieving with deionized water over a 63 micron meters mesh (e.g. Vautravers, Shackleton, Lopez-Martinez, & Grimalt, 2004). Initial size of bulk samples varied from ~1 to ~5 cm^3 for U1437B and were ~10 cm^3 for U1436C where larger samples were used because of the expected higher dilution by volcaniclastics. Because samples preparation on board Joides Resolution does not involve drying of the bulk sediment nor the settling of the fine fraction, when calculating the concentration per weight from the core catcher samples (i.e. treated during the cruise), the weight of <63 µm fraction had to be extrapolated from adjacent samples.

Studying the micropalaeontological content used a standard method (e.g. Vautravers et al., 2004) where most samples were sub-sampled using a micro-splitter followed by a dry-sieving step over a 150 µm sieve. The aim is for each sub-sample to contain c. 300 biogenic particles. However, at U1436 either due to very intense carbonate dissolution or dilution, this was impossible for some samples. Each subsample was spread on a gridded tray for identification of the planktonic foraminifers following the taxonomy of Kennett and Srinivasan (1983). All but non-biogenic particles (i.e. mostly

volcaniclastic particles) were counted. The biogenic particles categories are: (1) Individual planktonic foraminifer specimen per species (whole shell). (2) Planktonic foraminifer fragments (one fragment being less than half of a shell). (3). All benthic foraminifers were grouped together including rare broken ones. Each sub-sample was placed into a micropalaeontological slide for reference and imaging.

Stable isotopes analyses were performed on the shallow dwelling (<50 m water depth) and chlorophyll maximum feeder species *Neogloboquadrina dutertrei*, which is common to abundant in the sediments (Tamura et al., 2015) from 20 hand-picked specimens in the 250–300 µm size fraction. These samples were also used for the shell weights. Data and resulting stratigraphy are presented Schindlbeck et al. (2018) for U1437B and Vautravers et al. (2016) for U1436C.

4.3. Individual N. dutertrei *250–300 µm shell weight (SW)*

Shell weights (SW) were obtained by dividing the weight of *N. dutertrei* obtained on a high-precision scale (1 µg precision) in each of the sample picked for isotopic analyses by the number of shells. Within a relative narrow size range, SW provides reliable estimates of the amount of calcite per test. SW is an indicator of a combination of parameters, such as the calcification by the living foraminifer and the degree of dissolution after its death (Broecker & Clark, 2001).

4.4. Planktonic foraminifer (PF) assemblages

The study examined the fluctuations of five groups of species (polar–sub-polar, transitional, subtropical, tropical susceptible, and tropical resistant) expressed in percent of the total of whole planktonic shells counted. These groups were recognized by Thompson (1981) in the Northwest Pacific using a factor analysis method. Such faunal groups allow one species to belong to several factors. In some cases, these groups were slightly modified based on observations acquired in similar oceanic environments (i.e. in the Gulf Stream area) (Vautravers et al., 2004). Each group pertains to the palaeoceanographic goals as well as the reconstruction of the history of calcium carbonate preservation since two groups the tropical-susceptible and the tropical-resistant assemblages are recognized as opposite indicators on the carbonate preservation spectrum.

The polar/sub-polar group identifies the coldest intervals and traces the cold Oyashio current intrusions within the subtropical area during glacial intervals. Some other species (e.g. *Globoratalia menardii* and *Pulleniatina obliquiloculata*) are associated with strong western boundary currents (Bé, 1977; i.e. the Gulf-Stream and the Kuroshio) but are also tropical species part of the solution-resistant factor (Thompson, 1981).

Out of the 216 samples at U1436C, 15 contained less than 10 whole specimens and were excluded from the faunal associations study. However, they are part of the data-set investigating CD changes to not rule out that extreme low PF abundance results from dissolution. All samples from Hole U1437B were included in both parts of the study.

4.5. Carbonate dissolution proxies in the > 150 µm size fraction

The percent of planktonic foraminifer fragments (Pf) is a common proxy for dissolution is calculated following Howard and Prell (1994). The assumption being that tests become fragile before breaking and that the rate of breakage increases with dissolution.

The individual shell weight (SW) of *N. dutertrei* is used to confirm the $CaCO_3$ preservation status of the samples. Whilst Pf is often limited to later stages of dissolution (i.e. resulting in fragmentation) SW too has limitations but is an accepted proxy of CD (Broecker & Clark, 2001) probably more adapted for earlier stages of dissolution.

The number of whole planktonic foraminifer (nPF) per gram of dry bulk sediment is estimated from the counts of whole foraminifers divided by the weight of dry bulk sample. The rational behind this proxy is that as CD becomes more intense and then extreme the foraminifer shells break into

fragments and nPF in the coarse fraction above 150 µm decreases sharply tending towards and then reaching 0.

The ratio of whole benthic foraminifers to whole planktonic foraminifers (B/P) as a proxy of CD arises from selective solution of the various foraminifer shells. The rational implied behind this proxy is very similar to the progressive process leading to an over representation of the solution-resistant species amongst planktonic foraminifers. Such ratio is more valuable to estimate changes at one site rather than between sites because of differing local controls (i.e. productivity of the surface waters or water depth). Indeed, B/P can also be used to estimate productivity changes (Berger & Diester-Hass, 1988) especially at shallower depths.

The planktonic foraminifer simple species richness (SR) is the total number of PF morphospecies present in one sample, regardless of their abundances. In the course of increasing carbonate dissolution, the most sensitive PF species (Berger, 1968) are progressively removed and the percentages of solution-resistant species increase. It is therefore based on selective dissolution of the species. SR does not take into account each individual species abundances (but only their presence). Therefore, it is more appropriate in situations with extreme dissolution when all specimens from several sensitive species disappear. Outside this remit (i) SR decreases with temperature but with a lesser impact in the warm areas, where the number of species fluctuates less between glacial and interglacial. A modern subtropical/tropical assemblage at c. 30°N should have the highest SR, c. 23 species (Bé, 1977). Any sample with significantly lower SR demands an explanation either climatic (i.e. cold) or taphonomic.

5. Results

5.1. Planktonic foraminifers assemblages: Figure 2

The group "polar and subpolar" defined by Thompson (1981) contains *Neogloboquadrina pachyderma (sinistral)* and *(dextral)*, *Globigerina bulloides* to which *Turborotalita quinqueloba* and *Globigerinita uvula* are added (Figure 2(b)). At U1436C, the group varies between 0 and 60%. High values all found during glacials, MIS18 (28%), MIS12 (26%), MIS10 (38%), and MIS8 (23%). Apart from MIS9, which appears to be a very cold interglacial (36%) there is a tendency for interglacials prior to MIS17 to

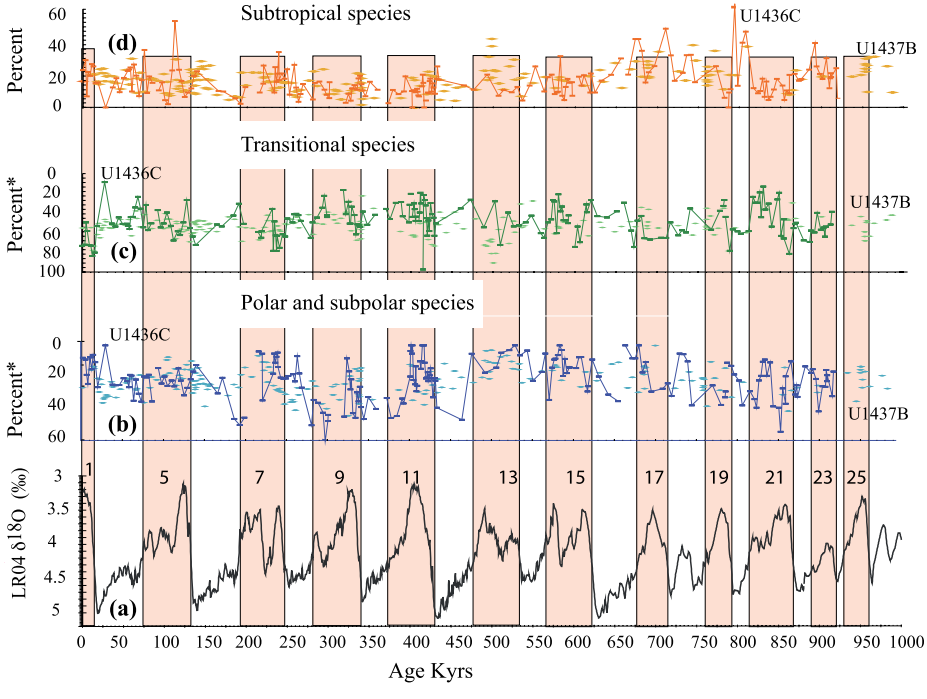

Figure 2. Faunal fluctuations. (a) $\delta^{18}O$ reference stack of Lisiecki and Raymo (2005), with interglacial intervals Marine Isotopic Stages (MIS) highlighted by pink bars and numbered from 1 to 25 (MIS were omitted for clarity); (b) Percentages of polar and subpolar planktonic foraminifers species on a reversed scale; (c) Percentages of transitional planktonic foraminifers species on a reversed scale; (d) Percentages of subtropical group of planktonic foraminifers species.

Notes: On panels b, c & d, the values for site 1436C are figured with dark colors and 1437B with light ones.

have higher values. MIS13 seems to be the longest, warmest interglacial if only based on this assemblage. Over the last 1 Ma, the observed range between averages is less than 3% between interglacials and glacials (20.5–23.3%) highlighting that the long-term changes are only subtle. At U1437B, the values range between 2 and 45%. Again, the longest and warmest interval is MIS13 (average of 13%). Although, temporal resolution is limited, earlier interglacial and glacial intervals (>700 ka) are, respectively, cooler and warmer than the later ones. MIS8 (33%) is the coldest glacial. The percentages observed for this group at U1436C contrast significantly with those are U1437B due to interglacials at U1436C being cooler and glacials warmer, respectively.

The transitional assemblage (Thompson, 1981) is dominated by *Globortalia inflata*, *Globorotalia truncatulinoides*, *Globorotalia crassaformis*, *N. pachyderma* (d), and *G. bulloides*. *Orbulina universa* was also added to the group (Figure 2(c)). At U1436C, the amplitude of variability is extreme (2–91%). This factor is the dominant one, averaging 51%. Values are much higher during glacials than interglacials and there is no significant trend observed along the record. Despite the tendency for higher values during interglacials (e.g. MIS21, 62%; MIS11 and 9, 59%) some isolated high values occur during glacials (e.g. MIS16 or MIS3). At U1437B, the factor dominates with a lower average (46%) its range is also smaller (9–77%). Similarly to U1436C, the highest average is found for MIS21 (59%). Most glacials values are c. 46 to 50%.

The subtropical factor (Thompson, 1981) is composed of two species; *Globigerinita glutinata* and *Globigerina falconensis*. The latter is added because it fluctuates similarly to *G. glutinata* and is reported elsewhere as part of subtropical assemblages (Bé, 1977). At U1436C, the group fluctuates between 0 and 63% (Figure 2(d)). However, it is the least represented group with only 15% on average over the last 0.9 My. The values for this group tend to be higher during glacial intervals, although there are isolated higher values during interglacials. Averages are 16% for interglacials and 20 for glacials. Higher values tend to be observed prior to 0.65 Ma. At U1437B, the range for the subtropical group is less than at U1436C (0–42%). The average over the whole data-set is 17%. Interglacial and glacial values are very similar. Higher values at U1437B are observed prior to 0.65 Ma, at this site the maximum is also lower (<40%).

5.2. Faunal-based proxies of carbonate dissolution: Figure 3

The **tropical susceptible factor** (Figure 3(b)) includes *Globigerinoides ruber* (white and pink), *Globigerinoides sacculifer* (with and without sac chamber) *Globigerinella aequilateralis, Globigerinella calida,* and *Globigerinita glutinata,* (Thompson, 1981), to which the rare *Globigerinoides tenellus and Globigerina rubescens* are added. At U1436C, the group varies between 0 and 68% representing on average 24% of total. At U1436C the group is more abundant during glacial stages (max MIS20, 48%) and often records high values towards the end of glacial stages. At U1437B, the fluctuations are similar but the range is less (56%) from 8% to 64%. The range between interglacial and glacial averages is also much less (1%). Interglacial average value (27%) is marginally higher than the glacial one (26%).

The **tropical-resistant factor** (Figure 3(c)) contains species with robust, often compact and thick shells: *N. dutertrei* and *P. obliquiloculata* and other species from the Globorotalia genus; *G. menardii, G. tumida, G. flexuosa, G. crassaformis, G. truncatulinoides*, and *G. hirsuta* as well as *Sphaeroidinella dehiscens*, (Thompson, 1981). This group exhibits the largest differences between sites. At U1436C, the range of values for the group is very large (0–40%) making it the second group recorded. However, the average for the whole data-set is only 19%. The glacials and interglacial averages are 16 and 20%, respectively. All values >12% are found during interglacials pointing to a strong taphonomic control at U1436C. For U1437B, the average for the whole data-set is only 7%, therefore significantly lower than at U1436C. The range observed from 0 and 22% is also considerably lower. All values > 7% are found during interglacials.

Planktonic foraminifers **simple Species richness** (SR, Figure 3(d)). At U1436C the average is 12 this may result from polar/sub-polar assemblage (Bé, 1977) with a lower diversity at the slightly

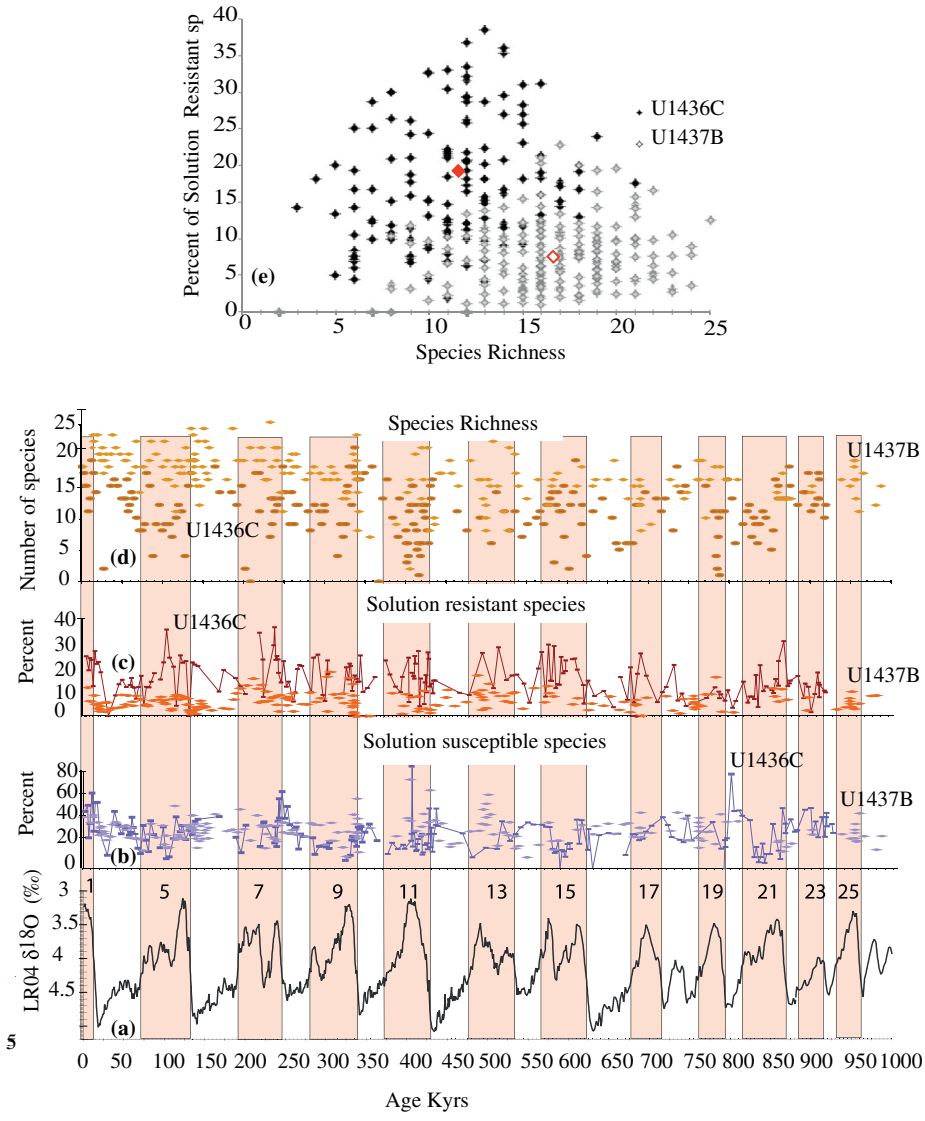

Figure 3. Faunal-based carbonate dissolution proxies. (a) $\delta^{18}O$ reference stack of Lisiecki and Raymo (2005) with interglacial intervals Marine Isotopic Stages (MIS) highlighted by pink bars and numbered from 1 to 25 (MIS was omitted for clarity); (b) Percentages of tropical solution susceptible planktonic foraminifers species; (c) Percentages of tropical solution-resistant planktonic foraminifers species. On panels b and c, the values for site 1436C are figured with dark colors and 1437B with light ones; (d) Species richness (1437B light color); (e) Percent of Solution-Resistant Species as a function of Species Richness for each site (empty diamonds 1437B, filled diamond 1436C), averages (red diamonds).

northward site. Seven glacials at U1436C (amongst 10) record values above the local average. Therefore, SR increasing rather than decreasing during glacial discounts colder surface water as the cause. SR values are generally lower during interglacials where other proxies pointed out the high level CD. This indicates that selective CD explains the SR pattern observed. There is also higher SR event presents during each glacial termination. At U1437B, the average SR is 16.7, therefore much higher than at U1436C. Although, it is possible that U1437B being located slightly south of U1436C maybe slightly warmer. The lowest SR recorded is found during interglacial MIS11 (SR = 2) indicating a very intense selective dissolution. The glacial–interglacial difference is small (0.4) compared to 1 for the other site but the pattern observed at U1436C (i.e. $SR_{glacial} > SR_{interglacial}$) is confirmed. Over 24 MIS, 6 are above the average of 16.7; MIS14, 8, 6, and 2 (4 glacials). More diversified assemblages are found in younger glacials after 0.6 Ma (i.e. end of MPT). The lowest SR (average 12.2) is observed for MIS17. SR averages and ranges are low during MIS11 at both sites as well as MIS17 at U1437B. A systematic higher SR event during most glacial terminations shows that there is a marked improvement in preservation at intermediate water depths in the Pacific Ocean. It is particularly obvious after MIS14 in the West of the Izu Ridge (1437B) and after MIS11 in the East.

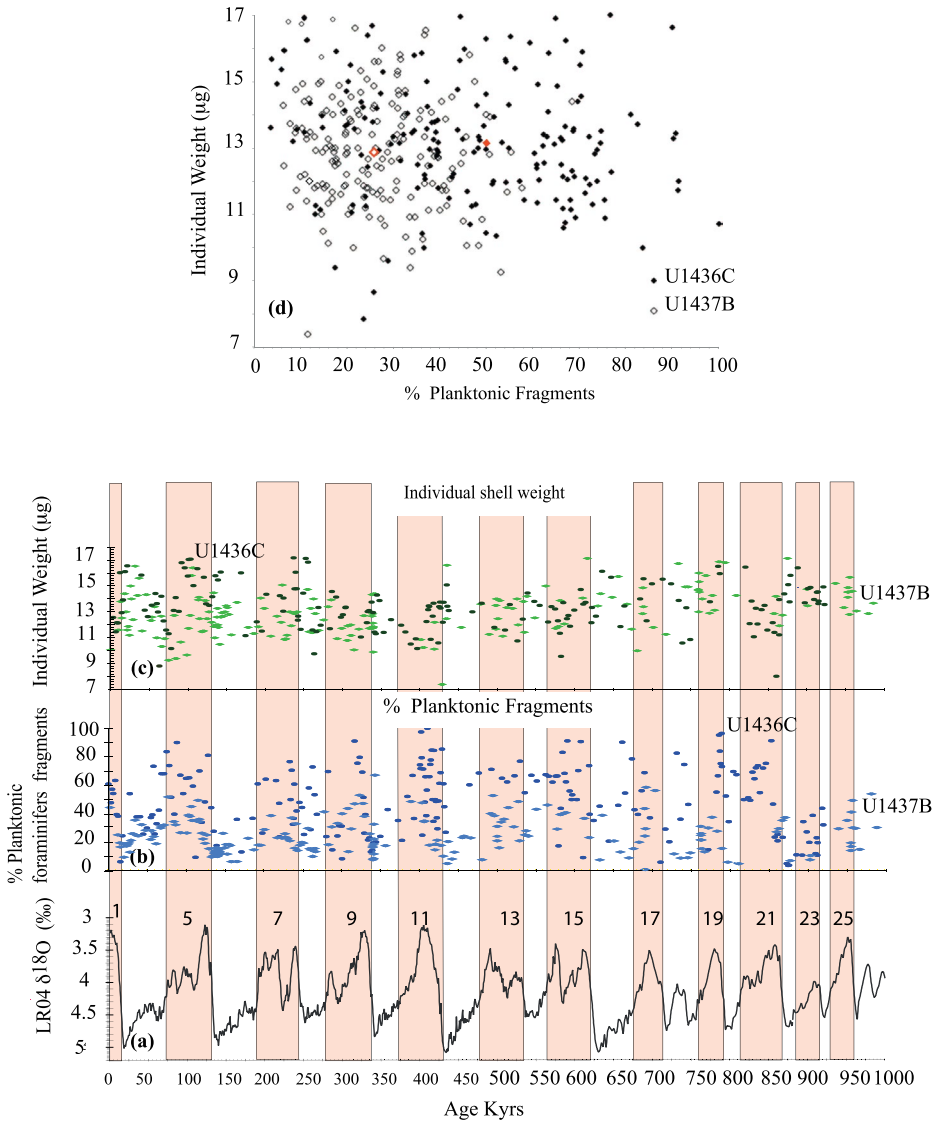

Figure 4. Shell-based carbonate dissolution proxies. (a) $\delta^{18}O$ reference stack of Lisiecki and Raymo (2005), with interglacial intervals Marine Isotopic Stages (MIS) highlighted by pink bars and numbered from 1 to 25 (MIS was omitted for clarity); (b) Percents of fragments of planktonic foraminifers at each Site; (c) Individual shell weight for *N. dutertrei* 250–300 µm. On panels b and c, the values for site 1436C are figured with darker colors and 1437B with lighter shades; (d) Individual shell weight as a function of percents of fragments for each site (empty diamonds 1437B, filled diamond 1436C), averages (red diamonds).

5.3. Individual shell-based proxies of Carbonate preservation

The **percentages of planktonic fragments** (Pf) (Figure 4(b)) experience extreme fluctuations at U1436C from 3 to 100%. High values are found during interglacials MIS11, 19, 21, 15, and 9 and the glacial MIS16. Twelve intervals have values above the overall average (i.e. 50%) and 9 of these are interglacials. MIS13 has the highest average. When a glacial has a high %Pf average (e.g. MIS16) the following interglacial has an even higher value. For the 21 MIS recorded, there is no exception. Nine intervals are <50% and 6 of these are glacials, MIS20, 16, 8, 2, and 6. Glacial values are less variable than interglacial. The drop in %Pf after any given interglacial is larger after 0.5 Ma. Also, glacial stages tend to record on average much better preservation after MIS11 (0.350 Ma) than prior, with two exceptions (MIS22 and MIS18). The average at U1437B (26%) is half that observed at U1436C (Figure 4(d)). However, even at 1437B; 11 MIS are above 26% and are more poorly preserved, 9 of these are interglacial stages. The interglacials values are within a narrow range c. 31%. The MIS17 interglacial (c. MPT) is poorly preserved. The "rule" that irrespective of the level recorded in the glacial Pf deteriorates in the succeeding interglacial holds here. Glacial PF assemblages are less fragmented during MIS20, 18, 12, 6, and 8. At U1436C, the most fragmented are found during MIS13, 19, and 5. Most interglacial experience a wide range of values (Figure 4). Glacial ranges are always lower

than interglacial ones. MIS14 is a glacial with a relative high level of dissolution as recorded by % Pf at both sites. MIS17 is one of the interglacials with the highest % Pf at both sites.

***N. dutertrei* shell weight** (SW) (Figure 4(c)) records an average of 13.2 µg at U1436C, the maximal values are found during MIS22 (14.7 µg), MIS5 (14.6 µg), and MIS16 (13.8 µg). Eleven marine isotopic stages have a SW above 13.2 µg of these, 6 are glacial stages. Similarly the tendency for higher SW and lower ranges is confirmed after MIS9 during interglacials. A further indication comes with the interglacial SW (14.4 µg) being higher than the glacial one (13.6 µg) at this site whilst the reverse (12.9 vs. 13.2 µg) is observed at U1437B. Therefore, there is only a very small difference despite very high evidence of dissolution during interglacial at U1436C. At U1437B, the average SW is lower (12.9 µg), although the range of values recorded is very similar from 7.4 to 17.1 µg (Figure 4(d)). The minimal value is found during interglacial MIS11 (10.9 µg) and fits with high % Pf. However, the SW averages are below average from MIS13 onwards. It would appear that SW works better at recording CD changes within the low CD intensity range. The maximal averages are found during the first part of the record, MIS20 at U1437B and during MIS22 at U1436C both with a value of 14.7 µg. Also, the absolute minimum average at both sites occurred during MIS11, the lightest 10.9 µg at U1437 and 11.8 µg at U1436C. This points to Site U1436C having experienced selective dissolution amongst *N. dutertrei* shells, which allows the average SW the species to show a minor and counter intuitive increase under intense dissolution. This probably arises from selective preservation of slightly larger shells picked although being sized between 250 and 300 µm in the more dissolved samples rather than more calcified tests.

5.4. Coarse fraction-based dissolution proxies

Whole benthic foraminifers/whole planktonic foraminifers ratio (B/P, Figure 5(b)). U1436C experiences extreme changes of this ratio (0–14). The average ratio is of 0.3 (3 benthic foraminifers' shells amongst 100 foraminifers). High values are found during MIS21, 19, 13, 11, 9, 7, and 5. Eight stages amongst 21 are above 0.3 and of these 7 are interglacial intervals. Eighteen samples have a ratio over 1, which means that they contain more benthic foraminifers than planktonic one. There seems to be no marked change of pattern anywhere along the 0.9 m.a. record. Again high ratio of B/P during interglacials traces intense dissolution at intermediate water depths. All, but one glacial stages have low values confirming the greatly improved preservation in every of U1436C glacial. At U1437B, the range of B/P is at least one order of magnitude smaller than at U1436C (i.e. 0–0.5 vs. 0–5). All, but four interglacial samples (MIS17, 9, 5) have a ratio under the average found at U1436C (0.07, or 7 benthics for 1,000 foraminifers). Nine intervals have an average above the general average of 0.07 and 6 out of these 9 are interglacials. The highest B/P ratios are found during the earlier part of the record MIS19, 11 for U1436C and MIS17 for U1437B. Similarly to the previous proxy (nPF/g), the ranges in B/P ratio are very large especially during interglacials.

Number of whole planktonic foraminifers/g (nPF, Figure 5(c)). Site U1436C average nPF is 1,646 per g, four of seven intervals above this value are glacial stages. More systematically during glacials after MIS13, the nPF always increases from one interglacial to the following glacial at the exception of MIS9-8. On average interglacial nPF is 1,554/g whereas the glacial value is 2,079/g. U1436C records a very large range of values from 0/g to 22,945/g. Although, values similar to 0/g could in some cases be explained by dilution by volcaniclastic large changes in preservation is the most likely explanation (Figure 5(d)). Another prominent and recurring feature is a systematic high nPF value c.10.000/g during an event at each glacial/interglacial termination. Such event is pervasive over the last 0.9 Ma and increases after MIS13. At U1437B, the average nPF is less with 695/g and the range is smaller between 4/g and 4,393/g. Over the last 1 My, only 4 MIS record values above the average and all of them are younger than MIS11. The Holocene records a drop below this average. A nPF termination event is also recorded at U1437B. The nPF tend to be poorly contrasted between climatic stages, especially prior to MIS17. U1436C (i.e. the most dissolved of the two sites) presents the highest concentrations. Significantly higher in average values (i.e. mostly due to glacial preservation) than at U1437B pointing to the existence of an additional factor boosting nPF during glacials

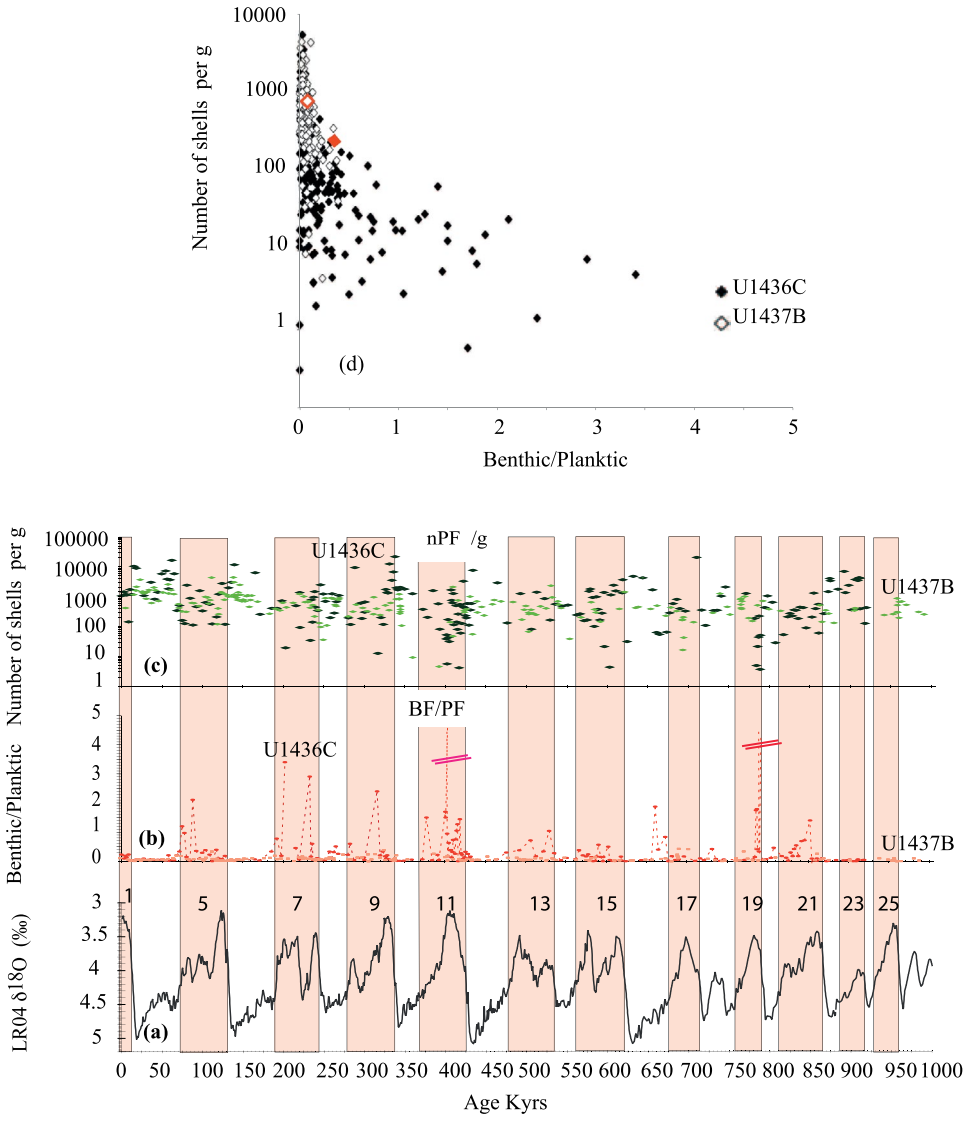

Figure 5. Coarse fraction-based carbonate dissolution proxies. (a) $\delta^{18}O$ reference stack of Lisiecki and Raymo (2005), with interglacial intervals Marine Isotopic Stages (MIS) highlighted by pink bars and numbered from 1 to 25 (MIS was omitted for clarity); (b) Ratio of whole benthic foraminifers over whole planktonic foraminifers (B/P) at each site (two samples are out of the scale >5); (c) All concentrations in whole planktonic foraminifers/gram at each site. On panels b and c, the values for site 1436C are figured with dark colors and 1437B with light ones; (d) Planktonic foraminifers concentration as a function of Benthic/Planktonic ratio for each site (empty diamonds 1437B, filled diamond 1436C), average (red diamonds). The two samples out of the scale at B/P >5 record PF concentration c. 1 per gram.

above the level recorded at U1437B. Local conditions for U1436C slightly northward in cooler and nutrients richer waters could explain part of the difference observed.

6. Discussion

U1436C and U1437B recorded a relatively continuous sedimentation in the area near the KC over the last 1 My. The higher sedimentation rate at U1437B (12 cm/ky) (Tamura et al., 2015). Schindlbeck et al. (2018) over this time interval results from (i) its location on fast accumulating sedimentary body and (ii) its lower overall rate of $CaCO_3$ dissolution, which has been assessed using a range of proxies. In the contrary, at Hole U1436C the average sedimentation rate is lower (~7 cm/ky) despite, based on sedimentary observations (Tamura et al., 2015) experiencing dilution by volcaniclastic particles.

Our observations of faunal assemblages indicate that selective dissolution (e.g. disproportionate representation of resistant species and decrease in number of species) during interglacials (Figure 3(c) and (d)) acted on many planktonic foraminifer assemblages in particular at U1436C (e.g. Figure 6(a)) despite recovered from a shallower water depth than U1437B. Fossils assemblages are therefore in some cases extreme distortions of living local assemblages. The quantitative faunal study of U1436C appears

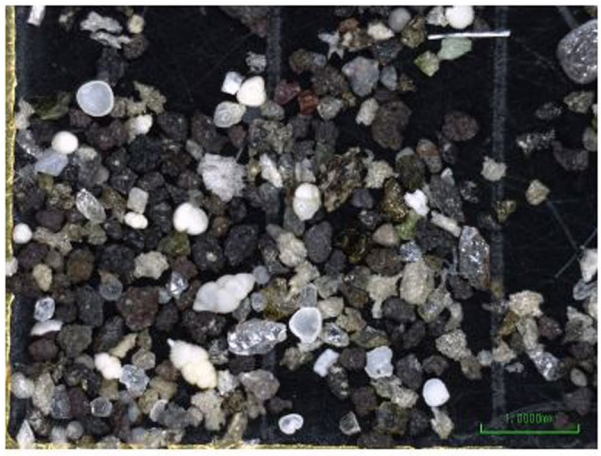

(a)

(b)

Figure 6. Two visual examples (×50) of very contrasted carbonate preservation styles recorded in the sediments coarse fraction (>150 micron meters). Also used on the cover. (a) Extreme case of carbonate dissolution at 1436C 4H2-56 cm found during interglacial MIS7 with high % planktonic fragments (76), high B/P ratio (2), high % of tropical-resistant species (36), low Species richness (7), low PF/gram, (8) and high shell weight (17). Also visible on the picture, numerous pumices and glass shards (mostly dark) diluting the biogenic fraction and dominating the lithogenic fraction; (b) Case of excellent carbonate preservation at 1437B 1H2-15 cm found during the last Glacial MIS2 with very low % planktonic fragments (10), very low B/P ratio (0.01), low% of tropical-resistant species (10), high species richness (23), high PF/gram (3667), and above average shell weight (14). Also present although less abundant than in (a) some light glass shards and pumices dominating the lithogenic fraction.

to yield a taphonomic record rather than a climatic one especially during interglacials. The strong CD makes this site less useful for palaeoclimatic reconstructions based on foraminifers including those based on trace metals analysis. For U1437B, the quality of the last 1 Ma record is overall good especially during glacials (e.g. Figure 6(b)) and only moderately biased by CD during interglacials.

6.1. Dissolution record, carbonate cycles and possible mechanisms

A numbers of CD proxies; based on foraminifer shells, their assemblages and their abundances in the coarse fraction were examined. All converge to identify high levels of CD during interglacials. Extreme carbonate dissolution is at work at U1436C more intensely than on the western side of the Izu Rise at U1437B. Both sites always experienced consistent changes in term of direction. Amongst all interglacials at U1437B, MIS17 is a rather remarkable one being the only during which the average value observed for the other site is reached. A preservation event is identified at both sites during glacial terminations and is more obvious after MIS17.

At U1436C, which experienced the higher level of CD throughout the last 0.9 My, there is a significant change affecting glacials after MIS11 (i.e. they record less dissolution). Interglacials continue to be intensively dissolved after MIS11, but they tend to be less so through time. Because this site is within the NPIW this can only be explained by a progressive yet major change with respect to carbonate chemistry in the global ocean. So, it would seem that the Pacific Ocean became more like the

modern Pacific in terms of carbonate cycles after MIS11 (i.e. typical interglacial CD and glacial preservation). The other known large change after MIS11 is the systematic occurrence of extreme swings in glacial and interglacial conditions including coincident large changes in sea-level (i.e. larger ice-sheets). This potentially indicates a connection between the global carbonate cycle and glacial–interglacial cycles. Similarly to the existence of a link between carbonate cycles and sea-level changes proposed by Hodell et al. (2001) as observed in the deep South Atlantic Ocean. At both sites, MIS11 shows a strong dissolution, a situation known yet poorly explained, at other intermediate water depth sites including the Caribbean Sea at ODP Site 999 (Schmidt, Vautravers, & Spero, 2006).

Changes recorded in sediments can illustrate contrasted carbonate saturation level between water masses or through time. This study helps to discriminate between two locations at relatively similar depths, far from the North Atlantic but where AAWI and NPIW are differentially influential and shows that if both sites are much less dissolved during glacials the site influenced by AAIW (U1437) is always less dissolved. Since AAIW operates as a conversion of NADW (Pahnke & Zahn, 2005) either changes in the input of dissolved carbonate upstream of AAIW during glacials (i.e. North Atlantic) or (and) increase rate of water circulation will be recorded in the area influenced by AAIW. This also would have applied to Glacial North Atlantic Intermediate Water (GNIW), which replaced NADW during glacials with a higher circulation rate (Freeman, Skinner, Waelbroeck, & Hodell, 2016). This could account for the preservation improvements found in glacial sediments at intermediate depths of the Caribbean (Schmidt et al., 2006) and North Atlantic (Thiagarajan et al., 2013) and is not antagonist with glacial deep Atlantic carbonate cycles (i.e. glacials are more dissolved) (Hodell et al., 2001) in the deepest part of the Atlantic. Indeed, in the deepest part of the ocean, AABW forming around Antarctica promotes CD during Glacials, whereas renewed or overshooting NADW circulation at glacial termination during some short-term glacial events drives enhanced carbonate preservation (Barker, Knorr, Vautravers, Diz, & Skinner, 2010). Glacial AABW formed under even more glaciated environment (i.e. more sea ice than today) could have accounted for an increased total CO_2 and helped explain the dissolution observed in the deepest Atlantic basins during glacials (i.e. contributing to explaining the Atlantic style of $CaCO_3$ cycle) as well as the stronger contrast with what is observed at intermediate depths.

The timing of changes (i.e. at the end of the MPT) points to an increasingly larger Laurentide ice-sheet from glacial MIS16 launching quantities of icebergs into the North Atlantic Ocean, which are traced by detrital carbonate rafted in middle latitudes (Hodell et al., 2008) as a potential cause. This, somehow, places larger ice-sheets as a potential actor on the carbonate system changes as recorded in the intermediate depths of the Pacific Ocean. In the one hand, the evidence of these coarse detrital carbonate (IRD) (Hodell et al., 2008), is just a fraction of all the detrital carbonate being injected into the ocean during melting events affecting the Laurentide either during deglaciations. In the other hand, evidence for rapid changes in carbonate preservation during each glacial to interglacial terminations. The resolution of this study does not permit investigation for similar rapid events elsewhere. However, in the area affected by the NPIW (U1436C), it is clear that each deglaciation and re-initiation of the NADW upstream of AAIW would seem to help preserved more carbonate in the North Pacific. However, at Site U1437 an even stronger change is visible during each glacials after MIS11. Although, outside the scope of this micropaleontological-based study and highly speculative, the addition of dissolved carbonate into the Glacial North Atlantic Water then transferred at each termination when NADW restarts its normal operation might explain observations. At U1437B, the onset of unusually high dissolution recorded during MIS17 suggests a sudden enhanced influence of NPIW over that of AAIW at the time. A lesser importance of AAIW during MIS17 has also been observed on the other side of the Pacific, off Chile by Martínez-Méndez et al. (2013). Because MIS17 has also lower CO_2 concentrations (i.e. milder interglacial) (Luthi et al., 2008) the interpretation that under intermediate interglacial climatic conditions the production of NPIW could be stimulated to become more important than AAIW as observed off Chile seems acceptable (Martínez-Méndez et al., 2013). In addition without trying to identify a cause for the low temperature during MIS17, it can be hypothesized that since the NPIW is a sink for carbon (i.e. storing some CO_2 in the Ocean) maybe an increased production of NPIW early in MIS17 would have helped atmospheric CO_2 to stay unusually low during MIS17. Further speculating, a cold MIS17 by maintaining larger than normal

interglacial ice could have led after MIS16 inception to the formation of an extremely large MIS16 NH ice-sheet, which is recorded by the benthic $\delta^{18}O$ (Lisiecki & Raymo, 2005). The later indicating the greater changes around the North Atlantic and the sudden larger involvement of the Laurentide ice-sheet into the northern hemisphere glaciation (Hodell et al., 2008). This study highlights the cool MIS17 interglacial as a pivotal moment when the subtropical West North Pacific was more influenced by NPIW and when NADW became more influential in the deep South Atlantic (Poirier & Billups, 2014). Either only concomitant or instrumental to higher ventilation at intermediate depth the development of a very large northern hemisphere ice-sheet could have somehow contributed to the reinforced "Pacific Carbonate Cycles", which is observed in this study starting from MIS17.

7. Conclusions

Based on a solid stable isotopic stratigraphy Vautravers et al. (2016), Kars et al. (2017), Schindlbeck et al. (2018) tied to LR04 Lisiecki and Raymo (2005), both sites appear to record a continuous although inter-bedded with ash sedimentation in the area of the Kuroshio over the last 1 Ma.

Identified by increases in the % of polar–sub-polar fauna during glacial intervals similarly to observation in the Gulf Stream area at a similar latitude (Vautravers et al., 2004) could trace the occurrence of cold events transmitted via the Oyashio cold current in an area normally occupied by the KC.

Two intervals MIS15-MIS13 and MIS5d-MIS1 stand out with unusually high amount of transitional species, suggesting that during milder climatic conditions, either moderate glacial or interglacial (i.e. MIS3 and MIS13) the transitional water may have greatly expended southward. This situation would have led to stronger than modern NPIW production consistent with the observation of increased CD especially at U1436C during MIS15-13.

Overall, the changes in the carbonate preservation record are consistent between the two sites. However, U1436C is always more affected than U1437B. Three intervals are recognized; prior MIS17, MIS17-MIS11, and after MIS11. The changes observed and the timing of onset from MIS16 implies a change within the GNAIW and point to either a change in the dissolved carbonate ions content during glacials (i.e. in the GNAIW) that could be related to the onset a periodic very large Laurentide ice-sheet from MIS16 onwards (Hodell et al., 2008) or to an enhanced rate of ventilation at intermediate water depth in the glacial Atlantic compared to modern similarly to what was found by Freeman et al. (2016) for the last glacial.

The interglacial MIS17 seems to be a pivotal time with the sudden increase in dissolution at U1437B signaling enhanced influence of NPIW. This change could have been driven by the enhanced production of NADW, which has been reported starting during this interglacial by Poirier and Billups (2014). An increased production of NPIW during the cool MIS17 could have helped store more CO_2 out of the atmosphere explaining relatively low CO_2 concentration (Luthi et al., 2008). This in turn could have triggered further extreme cooling during the next glacial (MIS16) explaining the steep change in ice volume at the time (i.e. the end of MPT).

From the next glacial MIS16 onwards, the Laurentide ice-sheet became larger and detrital carbonate (i.e. IRD) were first recorded (Hodell et al., 2008) in the middle latitude of the North Atlantic. Either only concomitant or instrumental to intermediate depth circulation globally the development of a very large NH ice-sheet could be seen as positive feedback on the "Pacific Carbonate Cycles".

Supplementary material

Data were obtained as part of a NERC–IODP moratorium grant and are also accessible on www.figshare.com. Table 1: Data for U1436C, Table 2: Data for 1437B.

Acknowledgments

My thanks go to the IODP staff sailing on *D/V JOIDES Resolution* during Exp 350. To professor David Hodell for giving me access to the Godwin Laboratory for Palaeoclimate Research facility, to the Department of Earth Sciences in Cambridge for hosting me. Special thanks to Suzanne Straub, Myriam Kars and Julie Schindlbeck for sharing samples. To Yoshi Tamura for Exp350, Peter Blum, Cathy Busby and Jim Gill for helping to improve a very preliminary version of the manuscript and to Manuela Bordiga for advice on figures. Thanks are also due the many reviewers of this work for their useful comments.

Funding
This work was supported by NERC UK-IODP [grant number NE/M005178/1].

Author details
Maryline J. Mleneck-Vautravers[1]
E-mail: mv217@cam.ac.uk
ORCID ID: http://orcid.org/0000-0003-2534-219X
[1] Godwin Laboratory for Palaeoclimate Research, Department of Earth Sciences, University of Cambridge, Downing Street, Cambridge CB2 3EQ, UK.

Citation information
Cite this article as: Quantitative planktonic foraminifers taphonomy and palaeoceanographic implications over the last 1 My from IODP Sites U1436 and U1437, Maryline J. Mleneck-Vautravers, *Cogent Geoscience* (2018), 4: 1447263.

Cover image
Source: Author.

References

Arhenius, G. (1953). Sediment cores from the East Pacific: Swedish deep sea expedition. *Geologiska Föreningen i Stockholm Förhandlingar, 75*(1), 115–118. https://doi.org/10.1080/11035895309454862

Barker, S., Knorr, G., Vautravers, M. J., Diz, P., & Skinner, L. C. (2010). Extreme deepening of the Atlantic overturning circulation during deglaciation. *Nature Geoscience, 3*, 567–571. https://doi.org/10.1038/ngeo921

Bé, A. W. H. (1977). A taxonomic and zoogeographic review of recent planktonic foraminifers. In A. T. S. Ramsay (Ed.), *Oceanic micropalaeontology* (vol. 1, pp. 1–100). New York, NY: Academic Press.

Berger, W. H. (1968). Planktonic foraminifera: Selective solution and palaeoclimatic interpretation. *Deep-Sea Research, 15*, 31–43.

Berger, W. H., & Diester-Hass, L. (1988). Palaeoproductivity: The benthic/planktonic ratio in foraminifera as a productivity index. *Marine Geology, 81*, 15–25. https://doi.org/10.1016/0025-3227(88)90014-X

Broecker, W. S., & Clark, E. (2001). An evaluation of Lohmann's foraminifera weight dissolution index. *Palaeoceanography, 16*(5), 531–534. https://doi.org/10.1029/2000PA000600

Driscoll, N. W., & Haug G. H (1998). A short circuit in thermohaline circulation: A cause for northern hemisphere Glaciation. *Science, 282*, 436–438. https://doi.org/10.1126/science.282.5388.436

Farrell, J. W., & Prell, W. L. (1989). Climatic change and $CaCO_3$ preservation: An 800,000 year bathymetric reconstruction from the central equatorial Pacific Ocean. *Palaeoceanography, 4*, 447–466. https://doi.org/10.1029/PA004i004p00447

Freeman, E., Skinner, L. C., Waelbroeck, C., & Hodell, D. (2016). Radiocarbon evidence for enhanced respired carbon storage in the Atlantic at the last glacial maximum. *Nature Communications, 2016*, 7. doi:10.1038/ncomms11998

Galbraith, E. D., Jaccard, S. L., Pedersen, T. F., Sigman, D. M., Haug, G. H., & Cook, M., ..., Roger, F. (2007). Carbon dioxide release from the North Pacific abyss during the last deglaciation. *Nature, 449*, 890–893. doi:10.1038/nature06227

He, Y., & White, W. B. (1987). Inter-annual variability of the Kuroshio frontal structure along its Western boundary in the North Pacific Ocean associated with the 1982 ENSO. *Journal of Physical Oceanography, 17*, 1495–1505.

Hodell, D. A., Channell, J. E. T., Curtis, J. H., Romero, O. E., & Röhl, U. (2008). Onset of "Hudson Strait" Heinrich events in the eastern North Atlantic at the end of the Middle Pleistocene transition (similar to 640 ka)? *Palaeoceanography, 23*(4), doi:10.1029/2008PA001591

Hodell, D. A., Charles, C. D., & Sierro, F. J. (2001). Late Pleistocene evolution of the ocean's carbonate system. *Earth and Planetary Science Letters, 192*(2), 109–124. doi:10.1016/S0012-821X(01)00430-7

Howard, W. R., & Prell, W. L. (1994). Late Quaternary $CaCO_3$ production and preservation in the Southern Ocean: Implications for Oceanic and atmospheric carbon cycling. *Paleoceanography, 9*(3), 453–482. https://doi.org/10.1029/93PA03524

Kars, M., Musgrave, R. J., Kodama, K., Jonas, A.-S., Bordiga, M., Ruesbam R., ..., Bauersachs, T. (2017). Impact of climate change on the magnetic mineral assemblage in marine sediments from Izu rear arc, NW Pacific Ocean, over the last 1Myr. *Palaeogeography, Palaeoclimatology, Palaeoecology, 480*, 53–69. doi:10.1016/j.palaeo.2017.05016

Kennett, J. P., & Srinivasan, M. S. (1983). Neogene Planktonic foraminifera. *A phylogenetic atlas*. Stroudsburg, PA: Hutchinson Ross publishing.

Le, J., & Shackleton, N. J. (1992). Carbonate dissolution fluctuations in the western equatorial pacific during the Late Quaternary. *Palaeoceanography, 7*(1), 21–42. https://doi.org/10.1029/91PA02854

Lisiecki, L. E., & Raymo, M. E. (2005). A Pliocene-Pleistocene stack of 57 globally distributed benthic $\delta^{18}O$ records. *Palaeoceanography, 20*. doi:10.1029/2004PA001071

Luthi, D., Le Floch, M., Bereiter, B., Blunier, T., Barnola, J.-M., Siegenthaler, U., ... Stocker, T. F. (2008). High-resolution carbon dioxide concentration record 650,000-800,000 years before present. *Nature, 453*, 1–5. doi:10.1038/nature06949

Martínez-Méndez, G., Hebbeln, D., Mohtadi, M., Lamy, F., Pol-Holz, D., Reyes-Macaya, D., & Freudenthal, T. (2013). Changes in the advection of Antarctic Intermediate Water to the northern Chilean coast during the last 970 kyr. *Palaeoceanography, 28*, 1–12. doi:10.1002/palo.20047

Orsi, A. H., Whitworth, T., III, & Worth, D. N., Jr. (1995). On the meridional extent and fronts of the Antarctic circumpolar current. *Deep-Sea Research, Part I-Oceanographic Research Papers, 42*, 641–673. https://doi.org/10.1016/0967-0637(95)00021-W

Pahnke, K., & Zahn, R. (2005). Southern hemisphere water mass conversion linked with North Atlantic climate variability. *Science, 307*, 1741–1746. doi:10.1126/science.1102163

Poirier, R. K., & Billups, K. (2014). The intensification of northern component deepwater formation during the mid-Pleistocene climate transition. *Palaeoceanography, 29*. doi:10.1002/2014PA002661

Qui, B. (2001). Kuroshio and Oyashio currents. In J. Steele, Thorpe, S., & Turekian, K. (Eds.), *Encyclopedia of ocean sciences* (pp. 1413–1425). Academic Press. doi:10.1006/nwos.2001.0350

Schindlbeck, J. C., Kutterolf, S., Straub, S. M., Andrews, G. D. M., Wang, K. L., & Mleneck-Vautravers, M. J. (2018). *The 1 Ma – Recent tephra record at IODP sites U1436 and U1437: Insights into explosive volcanism from the Japan and Izu arcs*. Arc Island. doi:10.1111/iar.12244

Schmidt, M. W., Vautravers, M. J., & Spero, H. J. (2006). Western Caribbean Sea surface temperatures during the late Quaternary. *Geochemistry Geophysics Geosystems, 7*. doi:10.1029/2005GC000957

Talley, L. D. (1993). Distribution and formation of North Pacific intermediate water. *Journal of Physical Oceanography, 23*, 517–537. https://doi.org/10.1175/1520-0485(1993)023<0517:DAFONP>2.0.CO;2

Talley, L. D. (2007). Hydrographic atlas of the world ocean circulation experiment (WOCE). In M. Sparrow, P. Chapman, & J. Gould (Eds.), *Volume 2: Pacific ocean*. Southampton: International WOCE Project Office. ISBN 0-904175-54-5. doi:10.21976/C6WC77

Talley, L. D., Nagata, Y., Fujimura, M., Kono, T., Inagake, D., Hirai, M., & Okuda, K. (1995). North Pacific intermediate water in the Kuroshio/Oyashio mixed water region. *Journal of Physical Oceanography, 25*, 475–501. https://doi.org/10.1175/1520-0485(1995)025<0475:NPIWIT>2.0.CO;2

Tamura, Y., Barker, A. K., Busby, C. J., Berger, J. L. R., Blum, P., Bongiolo, ... IODP Expedition 350. (2015). *Proceedings of the International Ocean Discovery Program, Expedition 350: Izu-Bonin-Mariana Rear Arc*. College Station, TX: International Ocean Discovery Program. https://doi.org/10.14379/iodp.proc.350.2015

Thiagarajan, N., Gerlach, D., Roberts, M. L., Burke, A., McNichol, A. P., Jenkins, W. J., ... Adkins, J. (2013). Movement of deep-sea coral populations on climatic timescales. *Palaeoceanography, 28*. doi:10.1002/paleo.20023

Thompson, P. R. (1981). Planktonic foraminifers in the Western North Pacific during the past 150,000 years: Comparison of modern and fossil assemblages. *Palaeogeography Palaeoclimatology Palaeoecology, 35*, 241–279. https://doi.org/10.1016/0031-0182(81)90099-7

Vautravers, M. J., Barker, A. K., Busby, C. J., Berger, J. L. R., Blum, P., Bongiolo,... Yang. (2016). Data report: Pleistocene planktonic foraminiferal Oxygen and Carbon stable isotopes records and their use to improve the age model of Hole U1436C recovered East of the volcanic Aogashima Island. *Proceedings of the International Ocean Discovery Program, 350*. doi:10.14379/iodp.proc.350.201.2016

Vautravers, M. J., Shackleton, N. J., Lopez-Martinez, C., & Grimalt, J. O. (2004). Gulf-Stream variability during MIS3. *Palaeoceanography, 19*. doi:10.1029/2003PA000966

White, W. B., & McCreary, J. P. (1976). On the formation of the Kuroshio meander and its relationship to the large-scale ocean circulation. *Deep Sea Research and Oceanographic Abstracts, 23*(1), 33–47. https://doi.org/10.1016/0011-7471(76)90806-8

Zeebe, R. E., & Marchitto, T. M. (2010). Atmosphere and ocean chemistry. *Nature Geoscience, 3*, 386–387. doi:10.1038/ngeo882

***Cogent Geoscience* (ISSN: 2331-2041) is published by Cogent OA, part of Taylor & Francis Group.**